

EVOLUTION OF AN ACTIVE REGION AND ASSOCIATED $H\alpha$ ARCH STRUCTURES

A. A. GEORGAKILAS

Section of Astrophysics, Astronomy and Mechanics, Department of Physics, GR-15784 Athens, Greece

TH. G. ZACHARIADIS

Research Center for Astronomy and Applied Mathematics, Academy of Athens, GR-10637 Athens, Greece

and

C. E. ALISSANDRAKIS

Section of Astrophysics, Astronomy and Mechanics, Department of Physics, GR-15784 Athens, Greece

(Received 26 October, 1992; in revised form 21 January, 1993)

Abstract. We have studied the early stages of development of two adjacent active regions observed at the center and the wings of $H\alpha$ for six days. From the growth of spots and arch structures we found that periods of slow flux emergence were followed by periods of vigorous flux emergence. We observed arch filaments covering an appreciable range of sizes (from a length of about 27 000 km and a height of 2000–3000 km to a length of 45 000 km and a height of about 15 000 km). Individual arch filaments within the same arcade sometimes have different inclinations of their planes with respect to the vertical. We observed isolated cases of arches crossing each other at an angle of $\sim 45^\circ$. During their early stages arch filament systems are short and they expand at a rate of about 0.8 km s^{-1} . The rate of growth of arch filament systems is faster when the orientation of the flux tubes is nearly parallel to the equator. Our observations suggest that the early part of the evolution of individual arch filaments in a grown system is not visible; however, in a few cases we observed arch filaments appearing as dark features near one footpoint and expanding towards the other, with a mean velocity of about 30 km s^{-1} .

1. Introduction

Large active regions with several spots form from multiple emerging flux regions (EFR) that occur simultaneously or in quick succession within a few days (e.g., Zwaan, 1985; Zirin, 1988, p. 333). The early stage of development of active regions is characterized by the presence of a variety of arch-shaped fibrils tracing the lines of force of the magnetic field (Zirin, 1972). Arch filament systems (AFS) mark the newly emerged lines of force and are present as long as new flux emerges (Bruzek, 1967, 1969), whereas field transition arches (FTA) span older magnetic inversion lines of active regions, connecting opposite polarities (Zirin, 1972). The study of active region arch structures is important because they carry information on the structure of the magnetic field shortly before emergence and its configuration upon its break out. The interactions between flux tubes play an important role in the dynamics of active regions.

Normally developing spot groups have conspicuous AFS for about 3 days only

(Bruzek, 1967). The apex of the arches is located at a height of 4000–20 000 km (Bruzek, 1967; Chou and Zirin, 1988) and their length is about 30 000 km (Bruzek, 1967). The initial tilt of AFSs with respect to the equator is highly random, but systems living more than a day rotate until they take the ‘proper’ tilt, which is nearly parallel to the equator (Weart and Zirin, 1969; Weart, 1970a). In some cases AFS rotate rapidly (up to 20° in less than an hour; Weart, 1970) while Frazier (1972) reported a rotation by as much as 90° in three days. Some authors have considered the possibility that magnetic flux tubes of arch filaments (AF) are twisted (Weart, 1970a, b, 1972; Glackin, 1975), however no clear observational evidence has been given so far. Plasma flows are observed within the flux tubes delineated by the arches. The classical picture is that of descending flows near the footpoints and ascending motions near the apex (Bruzek, 1969; Chou and Zirin, 1988; Georgakilas, Alissandrakis, and Zachariadis, 1990).

Field transition arches are fibrils connecting regions of opposite polarity, when flux no longer emerges (Zirin, 1974; Prata, 1971). They are successors of AFS in larger sunspot groups which no longer produce conspicuous AFS (Bruzek, 1967). Their similarity in appearance to AFS arches and the fact that material often flows along the arches suggest that they are also flux ropes tracing the magnetic field lines (Zirin, 1974; Prata, 1971). FTA usually connect plage regions; in that case their length depends on the distance of the plage regions, with typical value of 15 000 km (Prata, 1971). Often FTA connect a spot with a plage of opposite polarity or even two spots of opposite polarity (Zirin, 1988, p. 163).

In some cases small arches connect adjacent plage regions of strong field. Prata (1971) named arches of that class ‘neutral-line arch rows’ (NAR). On lower resolution photographs NARs look like crooked active region filaments (ARF) separating bright plages, but their actual structural form consists of a long series of parallel, closely spaced dark fibrils, joining regions of opposite polarity (Prata, 1971; Zirin, 1974). The length of NARs is of the order of 4000 km or less. NARs connect regions of strong field while ARF lie between regions of weaker fields; sometimes NARs are replaced by regular filaments (Prata, 1971; Zirin, 1972). The principal difference between the NAR and the FTA appears to be their size. In general the material flows in FTA are not the same as in AFS; they are more complex and depend on the structure of the arches (Georgakilas, Alissandrakis, and Zachariadis, 1990).

Bruzek (1967) found a close association between Ellerman bombs (EB) and AFS. He found that, in young bipolar active regions, Ellerman bombs were located only in the interspot region occupied by the AFS, while he gave one case of a spot group which had neither a conspicuous AFS nor any bright point on one day, but both features were present on the following day. He suggested that the occurrence of Ellerman bombs at the same location as AFS depends on either the propagation of the field through the low chromosphere or the ejection of matter.

In this paper we analyze high-resolution $H\alpha$ observations of two adjacent active regions which developed into a large sunspot group. We study the evolution of the

regions for six days, the structural characteristics of AFS and FTA during that period and the succession of AFS by FTA. Furthermore, we study the relation of AFS to Ellerman bombs and the relations of AFS and FTA with the magnetic field.

2. Observations

The observations were obtained with a Halle $H\alpha$ filter (0.5 Å passband) mounted on the 50 cm 'Tourelle' refractor of the Pic-du-Midi Observatory (Rösch and Dragesco, 1980). The exposure time was $\frac{1}{15}$ s at the line center, while the scale on the film was 10.5'' mm⁻¹.

A complex of two large developing active regions (with the single McMath No. 16315) was observed for six days from September 25 to September 30, 1979. The first day of our observations the region contained only two well-developed spots (Figure 1), while on the sixth day it had many large spots and its structure was quite complex.

On September 26 we obtained photographs at six positions along the $H\alpha$ line profile ($H\alpha$ center, $H\alpha \pm 0.5$ Å, $H\alpha \pm 0.75$ Å, $H\alpha \pm 1.0$ Å); the average duration of a scan, i.e., the time difference between successive photographs at the same wavelength was about 2 min while the region was observed for 80 min. On September 28 and 29 we obtained an 80 min long sequence of photographs at $H\alpha$ center; subsequent photographs were obtained within about 40 s. Occasionally we obtained photographs at $H\alpha$ and $H\alpha \pm 1.0$ Å, covering a period of about 6.5 hours and 4 hours, respectively. On September 25, 27, and 30 we occasionally obtained photographs at $H\alpha$ center and $H\alpha \pm 1.0$ Å, covering a period of about 10 min, 6.5 hours, and 4.5 hours, respectively.

According to *Solar Geophysical Data* (1981) the active regions produced on 1B flare on September 25, one 2B flare on September 30, and two 1N as well as one 1B flare on October 1. None of those occurred during our observations; we only had 3 small subflares on September 28 and one on September 29 (not reported in *SGD*), which did not produce any noticeable effects on the active region structure. We observed two more subflares (classified as -N in *SGD*) on September 30, near the end of our observations.

3. Active Region Evolution

The active region appeared on the east limb on September 20, 1979 and showed a very rapid growth. A few days later another region emerged nearby sharing the same neutral line. Within the next days the active regions developed into two large bipolar sunspot groups.

3.1. EVOLUTION OF SUNSPOTS AND PORES

During the first day of our observations (September 25) the south active region which appeared first (AR I from now on) consisted mainly of two well-developed

spots with penumbrae (spots *A* and *B*, Figure 1(a)) in its leading side and two pore regions (*C* and *D*, Figure 1(a)) at the other side of the neutral line of the magnetic field. The north active region (AR II from now on) consisted of a small spot without penumbra (spot α , Figure 1(a)) and a pore (α_1 , in Figure 1(a)) in the leading side and three pores (α_2 , Figure 1(a)) in the trailing side.

On September 26 we observed intense activity in AR I, in particular between pore regions *C* and *D* where new pores appeared, while those that already existed the previous day were in the process of merging, forming sunspots. Penumbrae formed at the outer part of the group of pores, but not in the region between the pores. At the same time a portion of spot *A* broke up. In AR II we could not identify any of the spots of the previous day; two new spots (*b* and *c*, Figure 1(b)), as well as some pores are visible.

The observations of September 27 show the spot *D* which formed overnight by coalescence; it had a well-developed penumbra, except in regions adjacent to pores (mainly west of the spot, Figure 1(c)). The pores of region *C* also formed a spot, which moved towards spot *B* and merged with it to form a large spot. Spot *A* decayed further and broke into smaller spots which apparently moved towards spot *B*, with which they merged on the next day, in a manner similar to the magnetic flux inflow features (MFI) of type 2, described by Vrabec (1974). In AR II the situation is almost unchanged: spot *b* is almost at the same position, while spot *c* appears displaced; lacking intermediate observations we cannot tell whether this is a real displacement or spot *c* faded away and a new spot, c_2 , formed.

On September 28 there was a dramatic change in both ARs, characterized by vigorous emergence of magnetic flux. In AR I two new spots formed (spots *F* and *G*, Figure 1(d)) which define a new magnetic dipole, completely different from that defined by spots *B* and *D* and with a different orientation. In AR II a large spot with partially developed penumbra formed in the place of spot *c* (spot *e*, Figure 1(d)). At the other side of the inversion line we have two spots in region *d* and another two in region *f* (Figure 1(d)).

On September 29 spot *B* in AR I had grown considerably, apparently by merging with spot *F* of the previous day. At the location of spot *D* there were then two new spots (*H*, Figure 1(e)), produced by the interaction of spot *D* with newly formed pores. Flux continued to emerge between the north part of spot *B* and region *I* where new spots and pores formed continuously. In AR II, spot *d* is enhanced and enlarged. At the other side of the inversion line a new spot (spot *g*, Figure 1(e)) formed, adjacent to spot *e*. New flux emerged in the region between spot *g* and the south part of spot *d*, evidenced by the presence of numerous pores.

The last day of our observations was September 30. In AR I the spots in region *I* merged to form a single, large spot (Figure 1(f)). At the other side of the dipole, in region *J*, new spots formed. There was not much change in AR II, except for the further growth of spot *d*.

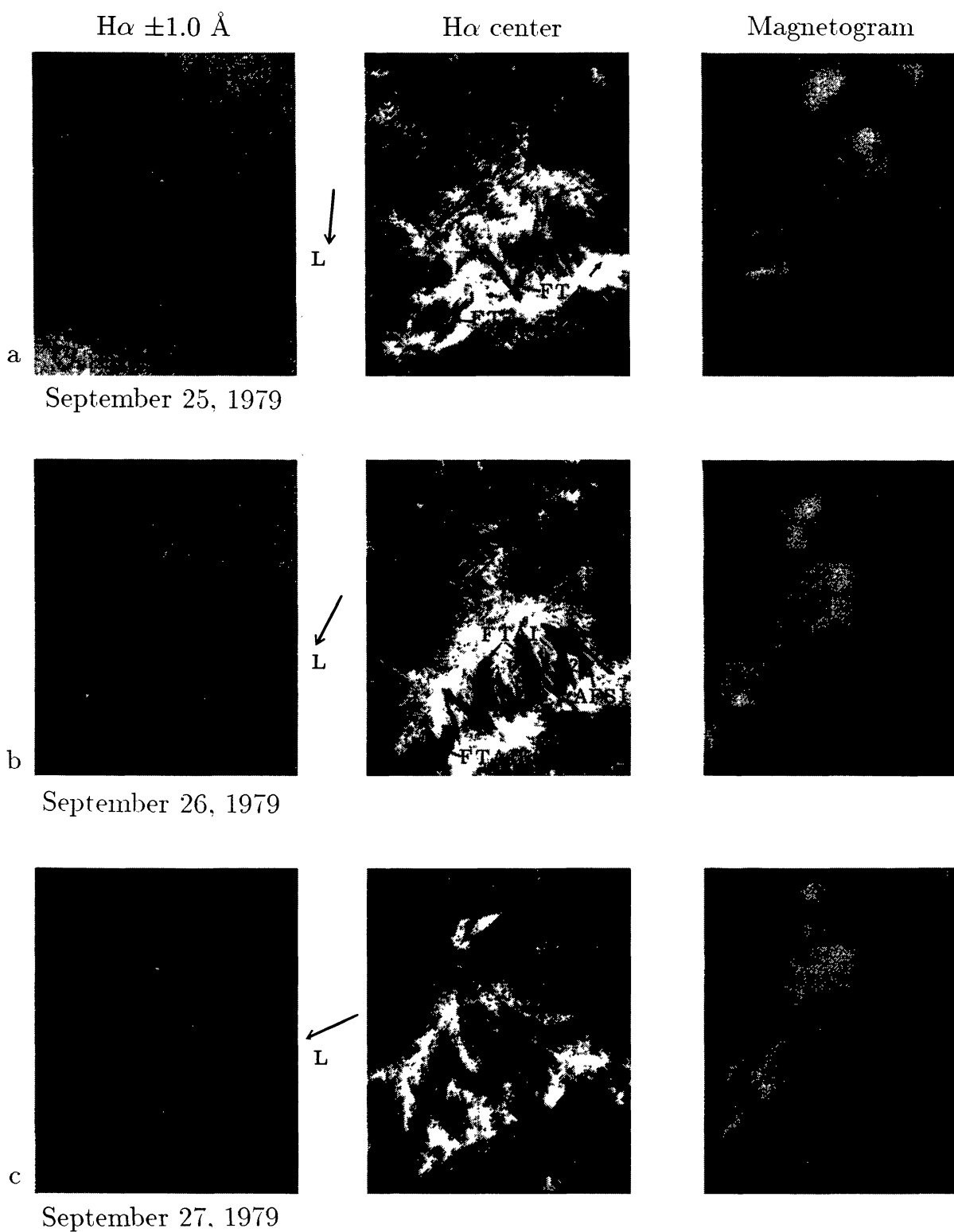


Fig. 1a-c.

Fig. 1. Photographs of the active region 16315 at $H\alpha \pm 1.0 \text{ \AA}$ and $H\alpha$ center together with Kitt Peak magnetograms on (a) 1979, September 25, (b) September 26, (c) September 27, (d) September 28, (e) September 29, (f) September 30. The length of the black line is $30''$. The photographs are oriented with the celestial west up and the celestial north to the left. The arrows marked W and L show the direction of the solar west and the solar limb, respectively.

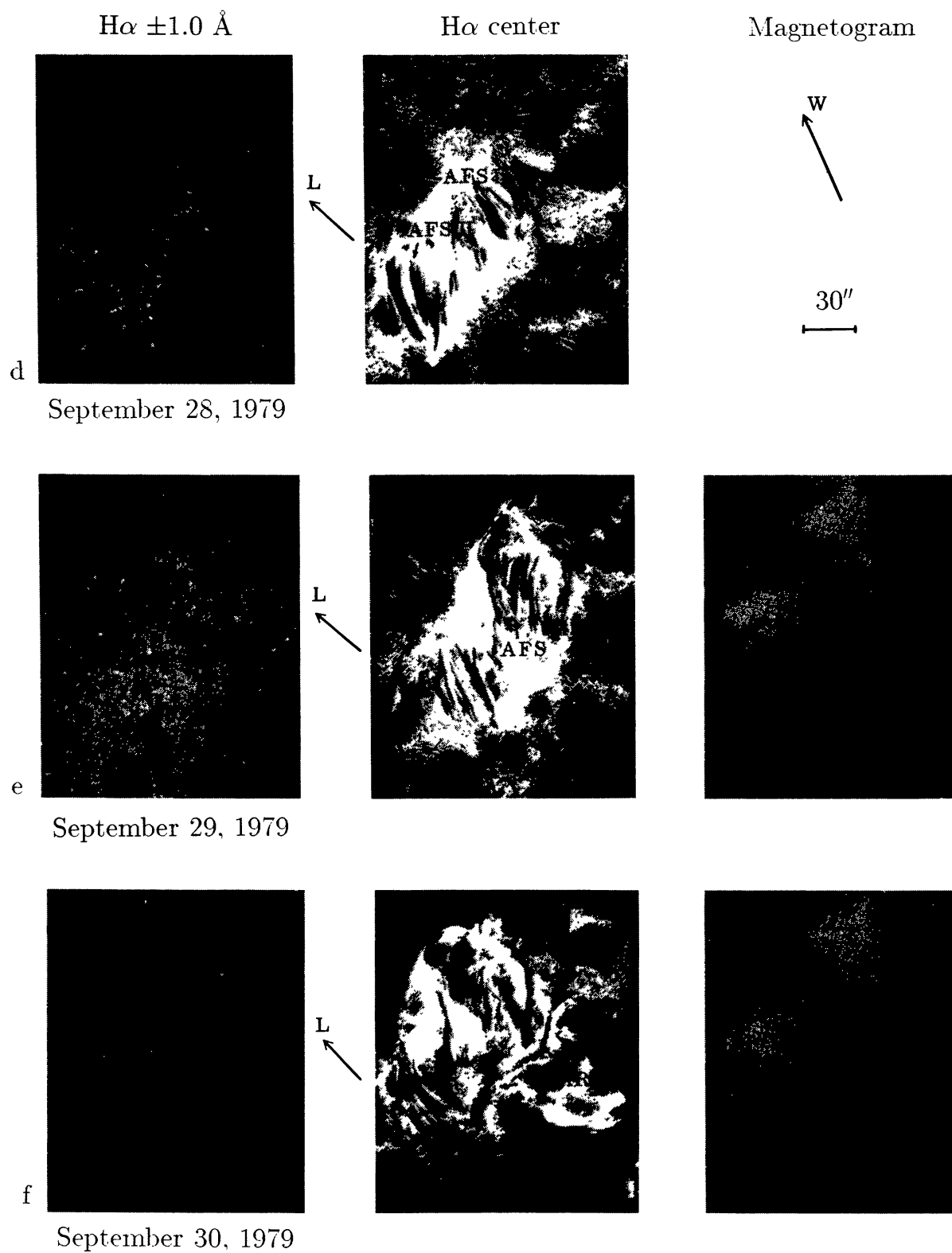


Fig. 1d-f.

3.2. EVOLUTION OF AFS AND FTA

On September 25 (Figure 1(a), at the time of our observations, FTAs extended mainly between pore regions *C* and *D* in AR I and between the small spot α and pore α_1 and the pores α_2 at the other side of the inversion line in AR II. No large spots were produced on that day and it appears that the emergence of flux was limited.

On September 26 (Figure 1(b)), arch filaments (AF) emerged in AR I between spots *C* and *D*; their structure and evolution, as well as the associated mass flow has been described by Georgakilas, Alissandrakis, and Zachariadis (1991). Under the arches we observed many intense EB. In AR II, less prominent AF were emerging between spots *c* and *b*. In both regions FTA developed next to the AF (FTA I, FTA II). The development of spots *C* and *D* suggests that there was considerable flux emergence in AR I while in AR II the spots remained relatively small, and it appears that the flux emerged at a low rate (cf. spot growth).

On September 27 (Figure 1(c)) FTAs succeeded the AFS in AR I. Most of them connected plages of opposite polarity, while some started from spot *C* and ended at distant plages or in the area just before spot *D*. In AR II a new AFS (AFS II) emerged between spots *c*₂ and *b*. The new configuration of spots *c*₂ and *b* was probably related to the emergence of the new AFS, which suggests the emergence of new flux. Next to the AFS, FTAs connected plages of opposite polarity; between AR I and AR II other FTAs connected extended plage regions.

On September 28 (Figure 1(d)) a new AFS developed in AR I, associated with the new spots *F* and *G*. The AFS emerged in a region occupied by FTAs in the previous day; the individual arches had the shape of a stretched S, an indication of twist. In AR II the AFS which were visible the previous day expanded considerably. They then connected spot *e* with the pair of spots in region *f*. From their length and the large size of spots produced, we conclude that flux emerged vigorously in AR II on that day.

On September 29 (Figure 1(e)) AFS appeared between spots *I* and *B* in AR I and between spots *d* and *g* in AR II. In both regions the AFS emerged between the FTA and it is difficult to distinguish between the two types of structures; they connected pores or young spots, located among the large old ones.

On September 30 (Figure 1(f)) FTA connected opposite polarities; the magnetic field configuration was very complex. NARs connected adjacent plages of opposite polarity. The length of the NARs changed with time (depending on the distance of the plage regions they connected) ranging from about 1800 km to about 3600 km at the same location. The NAR arches were very closely packed; at the time of their minimum length it was difficult to distinguish individual arches and the whole structure looked like a filament.

4. Orientation and Expansion of Arches

We have measured the length of AFS and their axial orientation and corrected them for projection effects. The length of the arches of AFS I (which had almost the proper E–W orientation) was about 36 000 km, which is comparable to the length of FTA I of the previous day. The arches did not appear to expand on that day. The FTA which succeeded the AFS on September 27 were about 42 000 km long.

Figure 2 shows the length and axial orientation of AFS II from September 25 to 29. The orientation of FTA II with respect to the E–W direction was about -65° on September 25 (measured northward from the west); the length of the longest fibrils was about 27 000 km. The associated magnetic dipole did not develop and did not produce any large spots on that day. On September 26 the dipole rotated by about 35° and its axial tilt became about -30° ; the length of the fibrils was the same as in the previous day. On September 27 the dipole assumed almost the ‘proper’ orientation (about -5°). The AFS which emerged on that day was initially about 18 000 km long (07:53 UT). During the day it grew rapidly at a rate of about 0.7 km s^{-1} ; at about 13:48 UT it was 33 000 km long (Figure 3), while on September 28 the length of the arches reached 48 000 km; they did not grow any further on that day. On September 29 their length decreased to 39 000 km.

The length of the arches of the new AFS which emerged on September 28 in AR I was about 33 000 km when we first observed them; they grew at a rate of about 0.5 km s^{-1} (Figure 4). The orientation of the dipole was not ‘proper’ and the fibrils were twisted by at least part of a full twist along their length. The dipole rotated by about 30° in one day (the initial rotation rate was about 2° per hour) until it assumed the proper tilt and the arches untwisted progressively.

5. Structure of Arches and Their Association with the Magnetic Field and Ellerman Bombs

The AFS, observed near the center of the disk, consisted of slightly curved filaments which converged near the footpoints and diverged at the top, suggesting lines of force of a magnetic dipole. Using the technique described in a previous paper (Georgakilas, Alissandrakis, and Zachariadis, 1990) we reconstructed the three-dimensional shape of arch filaments and we estimated the height of the apex above the footpoints as well as the inclination angle, β , of the loop plane with respect to the vertical. This technique assumes that the AFS were plane and symmetric with respect to their apex.

We reconstructed the shape of the bunches of arches 1 and 2 of AFS I on September 26 (Figure 1(b)). We note that bunch 2 was inclined to the opposite direction with respect to bunch 1. We found that the extreme values of the angle β of bunch 1 was about 45° and of bunch 2 about -6° ; the height of both bunches was about $6500 \pm 1500 \text{ km}$. From the reconstruction of bunches of AFS II on September 27 and 28 we found that β ranged between -5° and -20° and the height

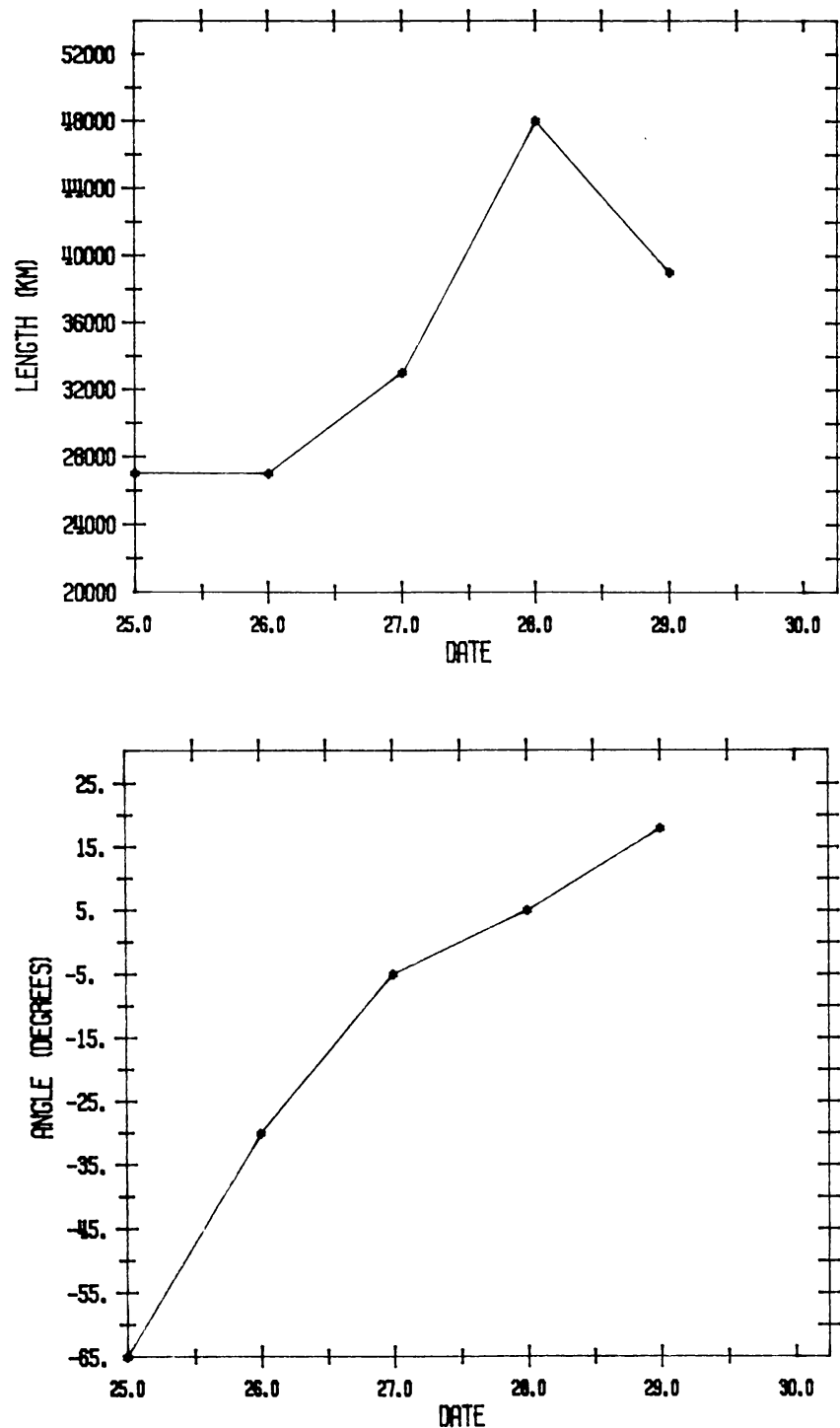


Fig. 2a-b. Length (a) and axial orientation (b) of AFS II from September 25 to 29, 1979.

of the arches ranged between 6500 km and 15 000 km. We could not reconstruct the shape of the bunches of AFS I on September 28 because of their twist. The method of reconstruction could not be applied to FTAs either, because their shape was either complex with threaded footpoints characteristic of fibrils delineating

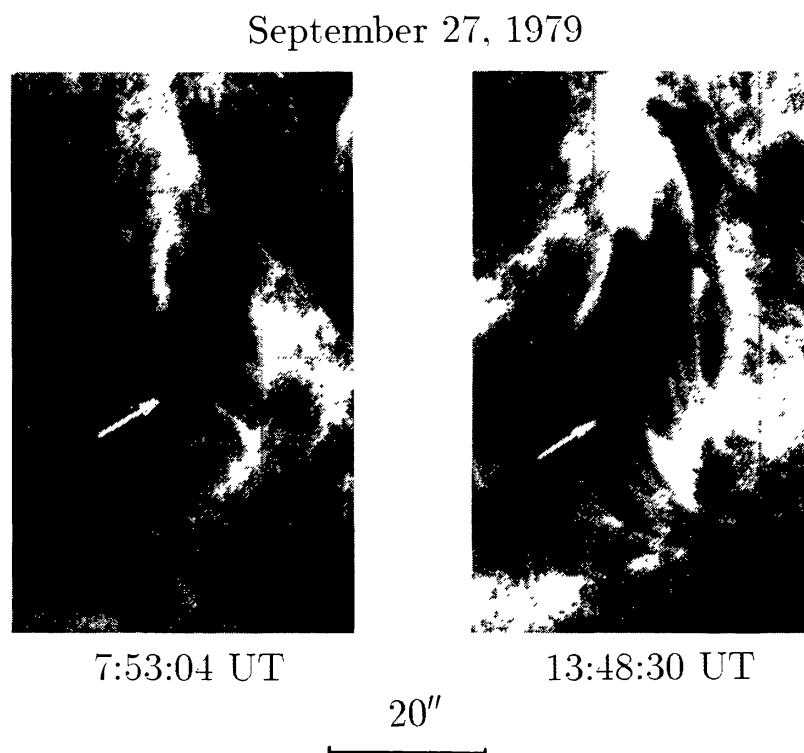


Fig. 3. Photographs of the active region on September 27, showing the development of AFS II.

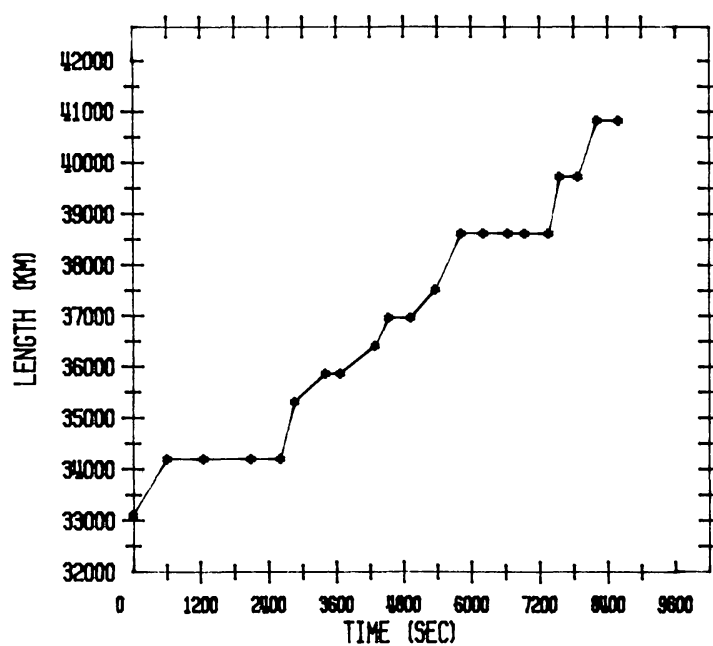


Fig. 4. The expansion rate of AFS I on September 28, 1979.

almost horizontal magnetic fields or slightly curved, with closely spaced parallel arches (Figure 1). The second case holds for rather short FTA and especially for NARs (Figure 1(f)).

In some cases we observed arches which apparently crossed with other arches.

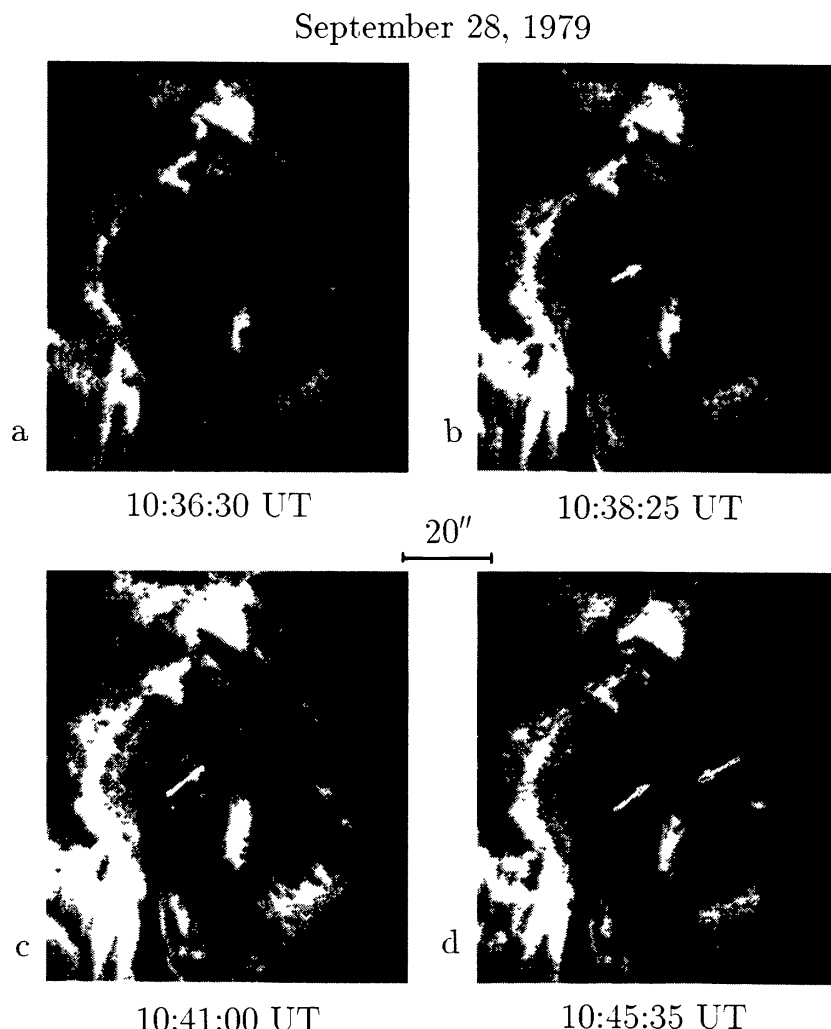


Fig. 5. Photographs on September 28 at the center of H α showing the appearance and evolution of arches which intersect with existing arches.

A characteristic example is shown in Figure 5(b). We note that there was no trace of the arch about 2 min earlier (Figure 5(a)). After another 7 min we observed another such arch (Figure 5(d)). Since these events were not followed by energy release, it is unlikely that the arches actually touched each other; most probably the arches were located at different heights, which indicates strong shear of the magnetic field along the vertical direction.

Arch filaments observed on the disk – as a rule – appear dark (in absorption) and have their footpoints in bright plage regions; quite often, however, their footpoints are bright at the line center (Bruzek, 1967). In a few cases we observed arch filaments which were bright, relative to adjacent dark filaments, along their full length (Figure 6). We could not tell whether the brightness difference was due to different physical conditions or there was a rarefaction of the fibrils at that location and thus they were fainter as seen against the bright background.

Both AFS and FTA connect regions of opposite polarity; however the neutral

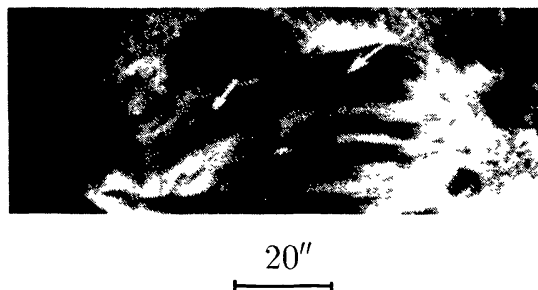


Fig. 6. Photograph on September 28 at the center of $H\alpha$ showing a bright arch filament.

line is not a straight line passing near the central part of the AFS. There is a dominant polarity (in our case it is the leading one) and the AFS (and some FTA) overlies 'peninsulas' of that polarity into the opposite polarity (Figure 1). These peninsulas usually end shortly before the footpoints of the AFS. Thus one footpoint of the AFS is near the neutral line while the other is located far into the opposite polarity. NARs span boundaries of opposite polarity and as the field becomes stronger they become shorter, darker, and more closely packed (Figure 1(f)).

During the six days of our observations we noticed that EB occurred under AFS, whereas we did not observe EB under FTA (Figure 1). Furthermore, we observed more numerous and intense EB at locations with intense flux emergence (Figure 1(d)). Thus it appears that there is a strong association between EB and flux emergence, which supports the suggestion of Zachariadis, Alissandrakis, and Banos (1987) that EB are the footpoints of low magnetic loops. We should note, however, that EB exhibit upward motions (Kurokawa *et al.*, 1982; Kitai, 1983) whereas the footpoints of AFS show descending motions.

6. Time Evolution of Individual Arches

We studied the $H\alpha$ time sequences on September 26, 28, and 29 in order to identify structural changes of arch structures with time scale of minutes. Although we often noticed structural differences of arch filaments in subsequent photographs, we rarely had the opportunity to observe the evolution of an individual arch filament from its birth. This is suggestive of the picture that new arch filaments form below the old ones and become visible when the latter expand and disappear; thus the early part of their evolution is not visible.

We noticed, however, a few cases where new arches appeared as dark features near one footpoint; subsequently the dark feature expanded towards the apex and further towards the other footpoint. A characteristic example is shown in Figure 7. The arch appeared as a darkening in the trailing (limbward) part of the active region and it was already about 11 000 km long in Figure 7(a). It reached the apex within about 12 min, with a mean apparent velocity of about 15 km s^{-1} ; at that time its length was about 22 000 km (Figure 7(b)). Subsequently it expanded towards the other footpoint and reached its maximum length of 44 000 km within about 7 min,

September 28, 1979

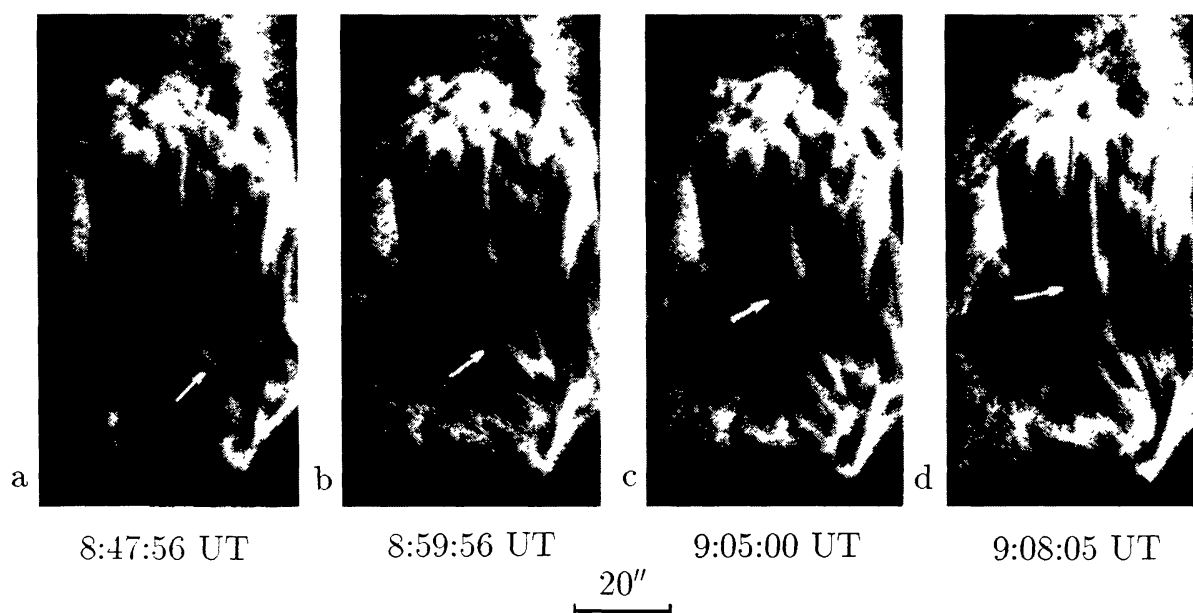


Fig. 7. Photographs on September 28 at the center of H α showing the appearance of arch 1 as a dark feature near one footpoint and its subsequent expansion towards the other.

with a mean velocity of about 43 km s^{-1} (Figure 7(d)). After reaching the other footpoint, it remained almost constant for about 11 min, and subsequently it began to fade; 1 min later only a few remnants were left, while two minutes later it had entirely disappeared. Its lifetime from the time it became observable to the time it began to fade was about 30 min. A similar evolution was observed in four other arches. Figure 8 shows their length as a function of time. The apparent expansion lasted for 10–25 min, with an average velocity of 15 to 30 km s^{-1} .

It is interesting to compare the evolution of the AF at the center of H α with mass motions derived from photographs obtained almost simultaneously in H $\alpha \pm 0.5 \text{ \AA}$. For this reason we selected a similar case from photographs obtained on September 26, when observations at H $\alpha \pm 0.5 \text{ \AA}$ were available. The arch filament began again from the limbward (east) footpoint and expanded towards the apex (Figure 9(a)). It reached the apex within about 2 min (between Figures 9(b) and 9(c)) and subsequently continued to expand towards the other footpoint; it reached its maximum length (about 30 000 km) within another 9 min (Figure 9(d)). The mean velocity of the expansion was 30 km s^{-1} . The photographs at H $\alpha \pm 0.5 \text{ \AA}$ showed that the mass motions associated with the arch were descending near the footpoint and ascending near its front (Figure 9(a)). This picture did not change when the arch reached the apex (Figure 9(b)). The part of the arch which expanded further from the apex to the other (western) footpoint showed ascending motions (Figure 9(c)), while when the arch reached its maximum length we observed descending motions near that footpoint (Figure 9(d)). Overall, the arch appears to exhibit the classical type of motion, with ascending material near the top and descending near the

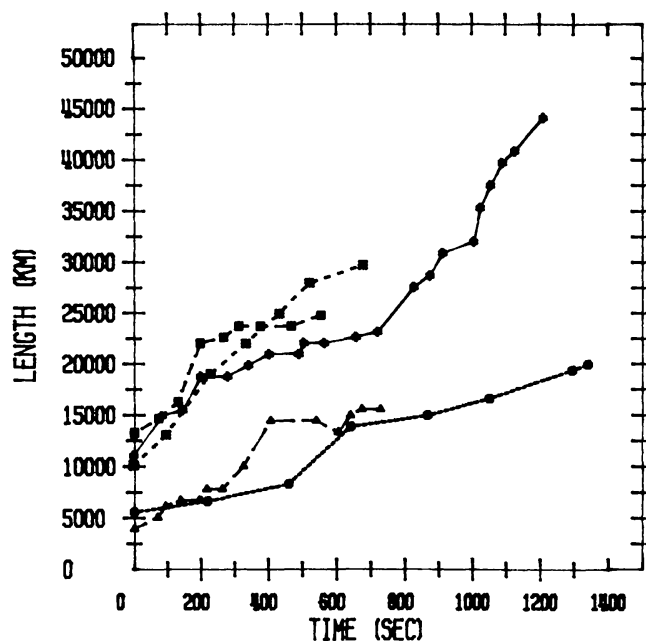


Fig. 8. The expansion rate of arches appearing as a dark feature near one footpoint and expanding towards the other.

footpoints of the arch loop. A similar case was presented by Tsiropoula *et al.* (1992).

The primary contradiction with the picture of an expanding structure, as seen at the line center, is the presence of descending material at the side where the expansion started. It is likely that the apparent expansion reflects a progressive change of physical conditions, such as cooling and/or density increase, rather than true material motion.

7. Summary and Conclusions

We studied the evolution of two adjacent active regions for a time period of six days: our emphasis was on the $H\alpha$ structures associated with the emergence of flux and the configuration of the magnetic field upon its break out from the subphotospheric layers. From the morphological study of the development of the active regions we conclude that the rate of emergence of the magnetic field is not constant: periods of slow emergence are followed by periods of fast emergence.

Our observations are consistent with results of previous authors (Weart and Zirin, 1969; Weart, 1970a), in that systems living more than a day rotate until they take the 'proper' orientation, which is nearly parallel to the equator. The rate of growth of AFS is faster when the orientation of the flux tubes is nearly parallel to the equator. In one case, while an AFS with twisted arches rotated towards the 'proper' orientation, individual arches untwisted progressively.

As a rule, arch filaments at the center of $H\alpha$ appear dark with bright footpoints; however, in a few cases we observed AF which were bright along their full length.

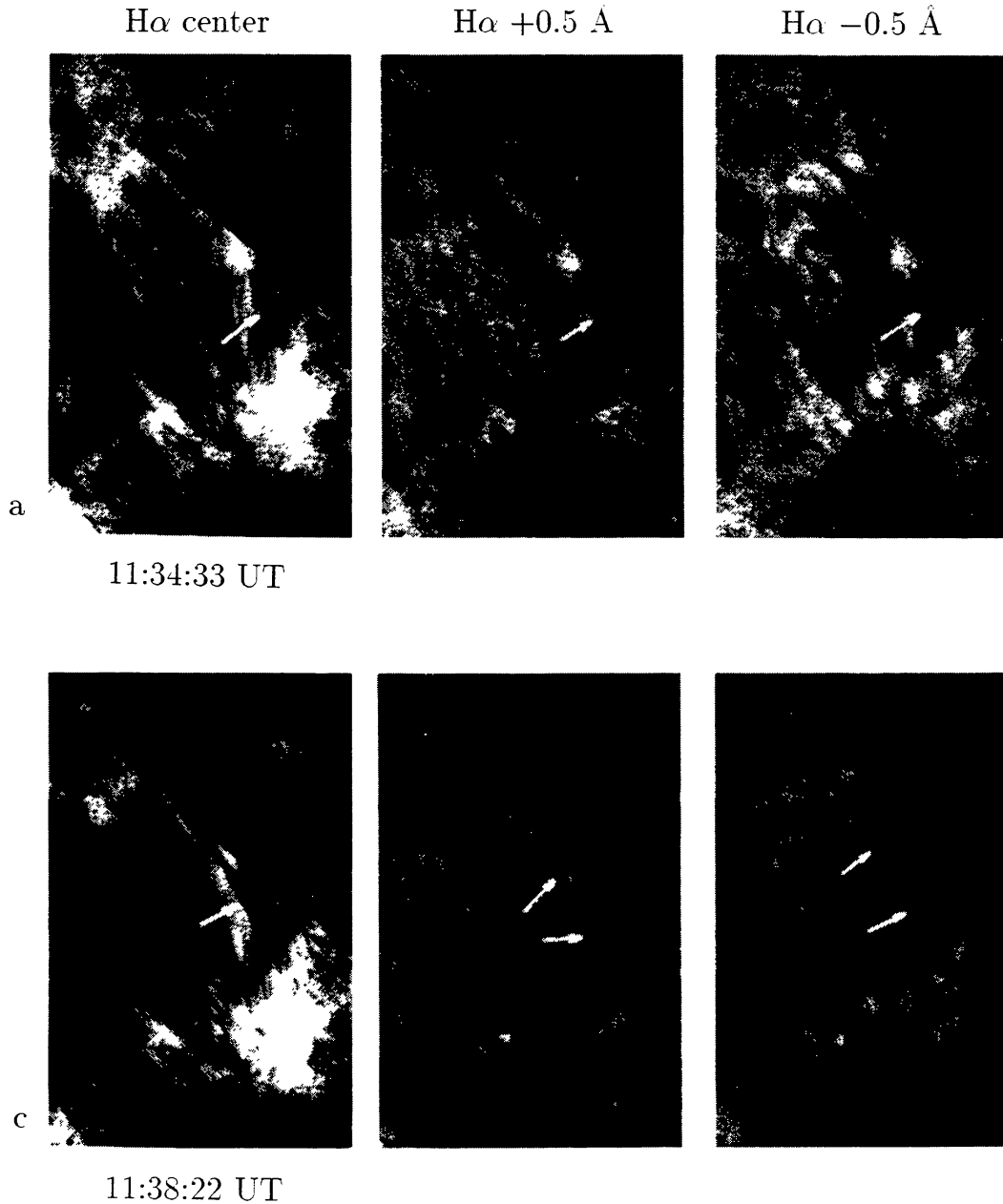


Fig. 9a, c.

Fig. 9. Photographs on September 26 at the center of $H\alpha$, $H\alpha + 0.5 \text{ \AA}$ and $H\alpha - 0.5 \text{ \AA}$ showing the expansion of arch 2 at the center of $H\alpha$ and the associated mass motions. The black line is $20''$ long.

This suggests that the physical conditions in individual arch filaments of the same arcade may vary considerably.

The size of arch filaments varies. We observed small arch filaments with a length of 27 000 km and a height of 2000–3000 km, medium size AF with a length of 35 000 km and a height of about 6500 km and large AF with a length of 45 000 km and a height of about 15 000 km. We actually observed even smaller AF which, however, were part of an expanding AFS. It appears that there is a relation

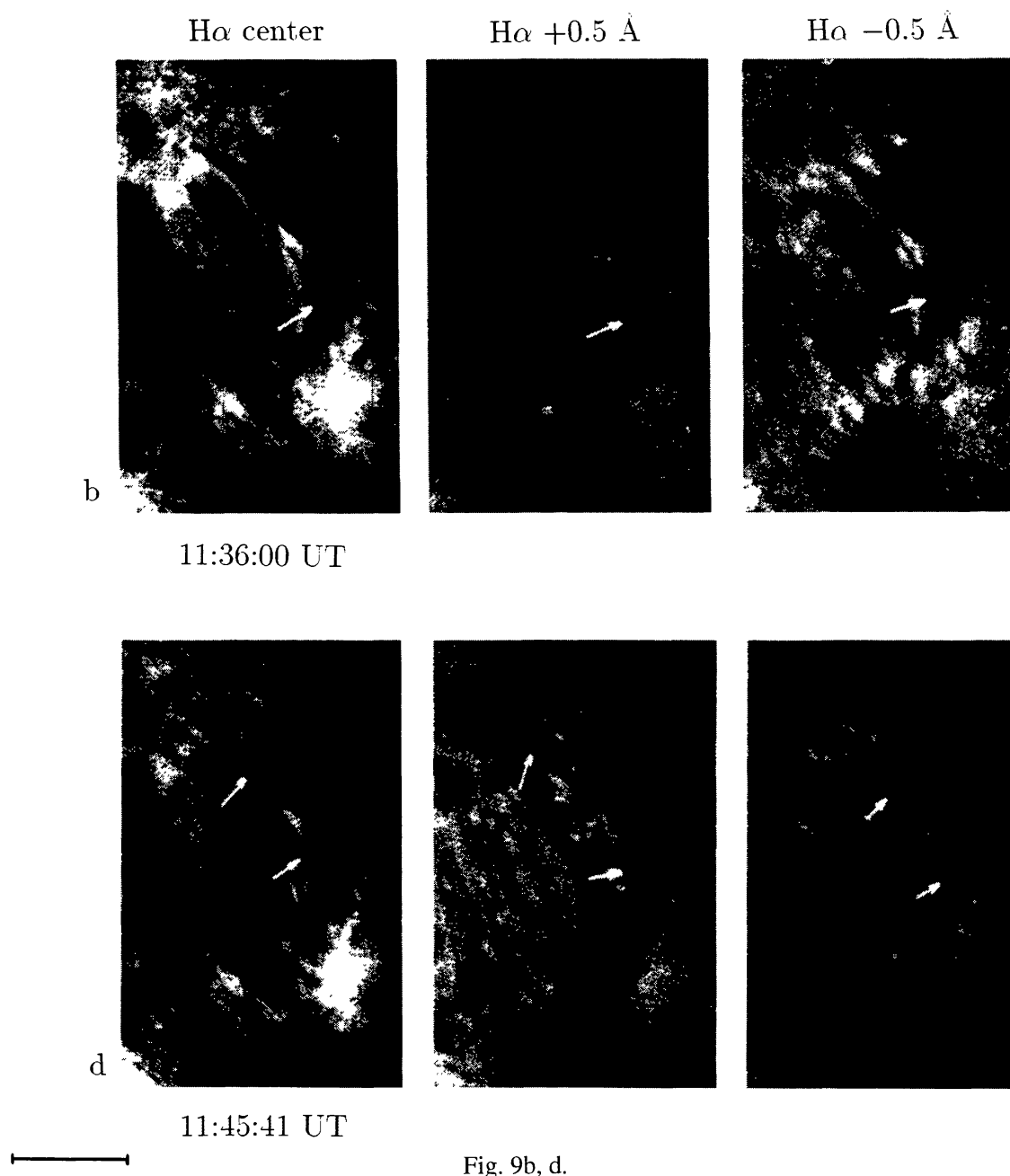


Fig. 9b, d.

between the height and the length of AF, shorter AFS being lower. The shape of AFS suggests that they consist of arch-shaped filaments which converge near the footpoints and diverge at the top. The inclination angle, β , of the loop plane with respect to the vertical for individual arch filaments of the same arcade varies; in one case it covered a range of 50° . Tsiropoula *et al.* (1982) found arch filament inclinations ranging from -40 to 50° in the same arcade. It appears that most AFS have arches covering an appreciable range of inclinations.

In some cases we observed arches which appeared to intersect with other arches. These events were not followed by any brightening, as would be expected if the arches actually touched and energy were released by magnetic reconnection. Most

probably the intersecting arches were located at different heights and their apparent crossing is a projection effect; in this case the intersection shows the presence of significant shear of the magnetic field along the vertical direction.

During the early stages the AFS are short and they expand at a rate of about 0.8 km s^{-1} . After reaching their maximum length they stop elongating further (at least appreciably) and continue to emerge with about the same length for hours. Vrabec (1974) found moving magnetic features instreaming towards each of the two sunspots of a bipolar group with velocities ranging from 0.25 to 1 km s^{-1} . Frazier (1972) measured the velocity of similar magnetic knots and found an average (transverse) speed of approximately 0.3 km s^{-1} . These measurements are in agreement with our measurements of the expansion rate of AFS and support the idea that the opposite moving magnetic features are the photospheric counterparts of the footpoints of arched magnetic flux tubes.

The structural changes of the arch filaments on a time scale of minutes suggest that new arch filaments from below replace the old ones and become visible when the latter expand and disappear. In a few cases we observed arch filaments at the center of $H\alpha$ to appear as dark features at one footpoint and subsequently expand towards the other footpoint with an average velocity of about 30 km s^{-1} . However, almost simultaneously photographs at $H\alpha \pm 0.5 \text{ \AA}$, showed the presence of descending material at the side where the expansion started. It is thus likely that the apparent expansion does not reflect true material motion, but rather a progressive change of physical conditions.

Usually AFS and FTA overlies intrusions of one polarity into the opposite; the intrusion ends shortly before the footpoints of the AF which is located within the opposite polarity. FTA which succeeded the AFS extended in the region of the innermost spots, which was occupied by the AFS as long as flux was emerging. Their length is comparable to the length of AFS. The shape of FTA is usually complex with threaded footpoints. As new flux emerged at about the same location, AFS push aside the FTA.

Ellerman bombs are closely related to AFS; we did not observe Ellerman bombs under FTA. Our observations support the idea of the association of EB with the footpoints of low magnetic loops. Frazier (1972) measured the velocity of individual magnetic knots and found an average (transverse) speed of approximately 0.3 km s^{-1} . These measurements are in good agreement with our measurements of the expansion rate of AF, taking into account that the expansion should be twice the velocity of individual knots. Zachariadis, Alissandrakis, and Banos (1987) found similar velocities for EB. These observations, together with the stopping of the expansion of AF after reaching a maximum length, supports the idea of the empirical model proposed by Frazier (1972): supergranular motions may bring flux tubes up to the surface and transport them laterally to the vertices of the cells.

Acknowledgements

One of the authors (C.E.A.) wishes to express his thanks to Prof. J. Rösch, Dr R. Muller, and the staff of the Pic-du-Midi Observatory for their invitation and warm hospitality. The authors wish to thank Prof. C. J. Macris for providing the H α filter and Dr Harvey for the Kitt Peak magnetograms.

References

- Bruzek, A.: 1967, *Solar Phys.* **2**, 451.
 Bruzek, A.: 1968, in K. O. Kiepenheuer (ed.), 'Structure and Development of Solar Active Regions', *IAU Symp.*, **35**, 293.
 Bruzek, A.: 1969, *Solar Phys.* **8**, 29.
 Chou, D.-Y. and Zirin, H.: 1988, *Astrophys. J.* **333**, 420.
 Frazier, E. N.: 1972, *Solar Phys.* **26**, 130.
 Georgakilas, A. A., Alissandrakis, C. E., and Zachariadis, Th. G.: 1990, *Solar Phys.* **129**, 277.
 Glackin, D. L.: 1975, *Solar Phys.* **43**, 317.
 Kitai, R.: 1983, *Solar Phys.* **87**, 135.
 Kurokawa, H., Kawaguchi, I., Funakoshi, Y., and Nakai, Y.: 1982, *Solar Phys.* **79**, 77.
 Prata, S. W.: 1971, *Solar Phys.* **20**, 310.
 Rösch, J. and Dragesco, J.: 1980, *Sky Telesc.* **59**, 6.
Solar Geophysical Data: 1981, No. 439, part II.
 Tsiropoula, G., Georgakilas, A. A., Alissandrakis, C. E., and Mein, P.: 1992, *Astron. Astrophys.* **262**, 587.
 Vrabec, D.: 1974, in R. G. Athay (ed.), 'Chromospheric Fine Structure', *IAU Symp.* **56**, 201.
 Weart, S. R.: 1970a, *Astrophys. J.* **162**, 987.
 Weart, S. R.: 1970b, *Solar Phys.* **14**, 274.
 Weart, S. R.: 1972, *Astrophys. J.* **177**, 271.
 Weart, S. R. and Zirin, H.: 1969, *Astron. Pacific* **81**, 270.
 Zachariadis, Th. G., Alissandrakis, C. E., and Banos, G.: 1987, *Solar Phys.* **108**, 227.
 Zirin, H.: 1972, *Solar Phys.* **22**, 34.
 Zirin, H.: 1974, in R. G. Athay (ed.), 'Chromospheric Fine Structure', *IAU Symp.* **56**, 161.
 Zirin, H.: 1988, *Astrophysics of the Sun*, Cambridge University Press, Cambridge.
 Zwaan, C.: 1985, *Solar Phys.* **100**, 397.